

Signature of multi-gap nodeless superconductivity in $\text{CaKFe}_4\text{As}_4$

P. K. Biswas,^{1,*} A. Iyo,² Y. Yoshida,² H. Eisaki,² K. Kawashima,³ and A. D. Hillier¹

¹*ISIS Pulsed Neutron and Muon Source, STFC Rutherford Appleton Laboratory, Harwell Campus, Didcot, Oxfordshire, OX11 0QX, United Kingdom*

²*National Institute of Advanced Industrial Science and Technology (AIST), 1-1-1 Umezono, Tsukuba, Ibaraki 305-8568, Japan*

³*IMRA Material R&D Co., Ltd., 2-1 Asahi-machi, Kariya, Aichi 448-0032, Japan*

A newly discovered family of high- T_c Fe-based superconductors, $A_e\text{AFe}_4\text{As}_4$ ($A_e = \text{Ca}, \text{Sr}, \text{Eu}$ and $A = \text{K}, \text{Rb}, \text{Cs}$), offers further opportunities to understand unconventional superconductivity in these materials. In this paper, we report on the superconducting and magnetic properties of $\text{CaKFe}_4\text{As}_4$, studied using muon spectroscopy. Zero field muon-spin-relaxation studies carried out on the $\text{CaKFe}_4\text{As}_4$ superconductor do not show any detectable magnetic anomaly at T_c or below, implying that time-reversal-symmetry is preserved in the superconducting ground state. The temperature dependence of the superfluid density of $\text{CaKFe}_4\text{As}_4$ is found to be compatible with a two-gap $s+s$ -wave model with gap values of 8.6(4) and 2.5(3) meV, similar to the other Fe-based superconductors. The presence of two superconducting energy gaps is consistent with theoretical and other experimental studies on this material. The value of the penetration depth at $T = 0$ K has been determined as 289(22) nm.

PACS numbers: 74.25.F-, 74.25.Ha, 76.75.+i

Recent years have witnessed huge research interest in Fe-based superconductors not only due to higher superconducting transition temperature, T_c , but also because of the unconventional superconducting properties and interplay with various electronic ground states, such as nematic phase, magnetism [1–5]. This family has a diverse range of structures all containing a common Fe_2An_2 ($\text{An} = \text{P}, \text{As}, \text{Se}, \text{Te}$) layer, analogous to the CuO_2 layers in high- T_c cuprates [6]. $A_e\text{AFe}_4\text{As}_4$ ($A_e = \text{Ca}, \text{Sr}, \text{Eu}$ and $A = \text{K}, \text{Rb}, \text{Cs}$) materials, discovered in 2016, are the new family of Fe-based superconductors with T_c of $\approx 31\text{--}36$ K [7]. Until now, only a few experimental studies have been performed which show that this new family of superconductors is structurally identical to CaFe_2As_2 , with the A_e and A sites forming alternating planes along the crystallographic c -axis, separated by FeAs layers [7]. Unlike other Fe-based superconductors, $A_e\text{AFe}_4\text{As}_4$ does not show any structural phase transition below room temperature [8]. However, Eu-containing $A_e\text{AFe}_4\text{As}_4$ show a magnetic transition at ≈ 15 K [9, 10]. Along with high T_c values, the $A_e\text{AFe}_4\text{As}_4$ family also show a very high upper critical field (≈ 92 T for $\text{CaKFe}_4\text{As}_4$) [11], similar to the optimally doped $(\text{Ba}, \text{K})\text{Fe}_2\text{As}_2$ [12] which is well above the Pauli paramagnetic limit $H_p(0) = 1.86 * T_c$ for weak-coupling BCS superconductors. Measurements of the London penetration depth $\lambda(T)$ using a Tunnel-diode resonator (TDR) and tunneling conductance from a Scanning tunneling microscope (STM) spectroscopy show two nodeless gaps in $\text{CaKFe}_4\text{As}_4$ with a larger gap of between 6-9 meV and a smaller gap of between 1-4 meV [13]. High-resolution angle-resolved photoemission spectroscopy (ARPES) measurements and density functional theory (DFT) calculations support multi-band superconductivity in $\text{CaKFe}_4\text{As}_4$, in which Cooper pairs form in the electron and the hole bands interacting via

a dominant interband repulsive interaction enhanced by Fermi surface (FS) nesting [14]. Other thermodynamic and transport measurements on $\text{CaKFe}_4\text{As}_4$, such as resistivity, thermoelectric power, Hall effect, magnetization, and specific heat, etc. all show similar properties to the optimally doped $(\text{Ba}_{1-x}\text{K}_x)\text{Fe}_2\text{As}_2$ [8]. This fully ordered and stoichiometric $A_e\text{AFe}_4\text{As}_4$ family of superconductors with high- T_c values therefore provide new and unique opportunities to test and compare the experimental and theoretical understanding of the Fe-based superconductors. In addition, the ordered nature of the structure makes theoretical models easier to develop. In this respect, it is of critical importance to understand the superconducting and magnetic properties of $\text{CaKFe}_4\text{As}_4$ and obtain detailed knowledge of the superconducting order parameters.

In this article, we report the results from muon spin rotation and relaxation (μSR) studies on the superconducting and magnetic properties of $\text{CaKFe}_4\text{As}_4$ at the microscopic level. We have investigated the symmetry of the superconducting gap of $\text{CaKFe}_4\text{As}_4$ by measuring the magnetic penetration depth as a function of temperature $\lambda(T)$. Our results show that $\text{CaKFe}_4\text{As}_4$ is a nodeless multi-gap superconductor with gap sizes of 8.6(4) and 2.5(3) meV. We also obtained the penetration depth at 0 K, $\lambda(0) = 289(22)$ nm. Using ZF- μSR technique we confirm that $\text{CaKFe}_4\text{As}_4$ is paramagnetic in the normal state. It further shows that the superconducting state of $\text{CaKFe}_4\text{As}_4$ preserves time-reversal-symmetry (TRS).

Polycrystalline samples of $\text{CaKFe}_4\text{As}_4$ were synthesized using the stainless steel (SUS) pipe and cap method described in ref. 7. Sample characterization measurements (not shown here) were performed at the National Institute of Advanced Industrial Science and Technology (AIST), Japan. Zero-field (ZF)- and transverse-

field (TF)- μ SR experiments were carried out using the MuSR spectrometer [15] at the ISIS facility, STFC Rutherford Appleton Laboratory, UK. Powder samples of $\text{CaKFe}_4\text{As}_4$ were pressed into 6 pellets of diameter 6 mm and thickness ≈ 1 mm each. For measurements in ZF-mode, a mosaic of the 6 pellets were mounted onto a 99.995% pure silver plate. Any muon stopping in the silver plate gave a constant background signal over the temperature range of interest. For the measurements in TF-mode, hematite slabs were positioned immediately behind the sample. Muons stopped in the hematite slabs depolarized immediately and hence the background in the data collected was significantly reduced. In the TF- μ SR experiments, 40 mT field was applied (above T_c) perpendicular to the initial muon spin polarization. The samples were then cooled to base temperature (1.5 K) in a magnetic field and the μ SR spectra were collected upon warming the sample. The typical counting statistics were ~ 30 million muon decays per data point. The ZF- and TF- μ SR data were analyzed using the free software packages Mantid [16] and MUSRFIT [17].

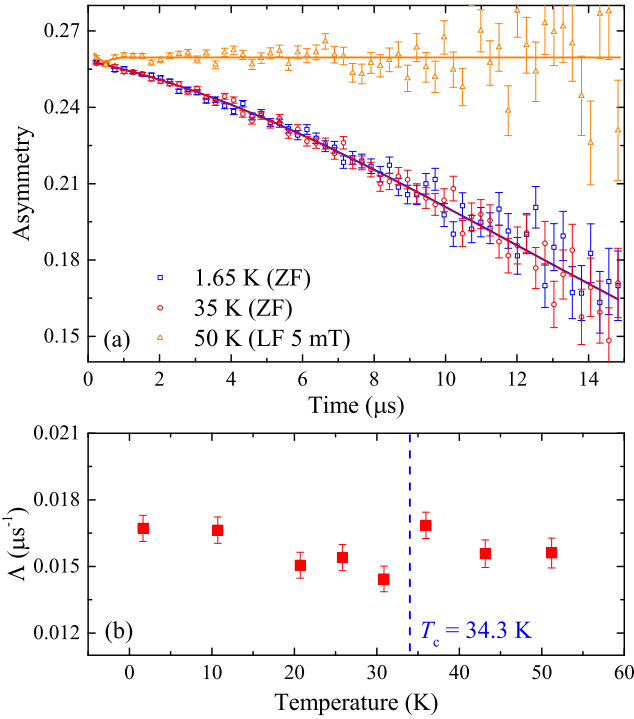


FIG. 1: (Color online) (a) Zero-field ($T = 1.65$ and $T = 35$ K) and longitudinal-field ($T = 50$ K and $\mu_0 H = 5$ mT) μ SR time spectra for $\text{CaKFe}_4\text{As}_4$. The solid lines are the fits to the data using Eq. 1, described in the text. (b) Temperature dependence of the muon spin relaxation rate Λ , extracted from the ZF- μ SR time spectra.

ZF- μ SR measurements were performed to investigate the magnetic properties of $\text{CaKFe}_4\text{As}_4$ superconductor, especially to look for any additional magnetic signal arising spontaneously with the onset of superconductivity,

associated with time-reversal-symmetry breaking fields. Figure 1 (a) shows the ZF- μ SR time spectra measured at $T = 1.65$ and 35 K. ZF data collected above and below T_c show negligible difference, implies that there is no additional relaxation of the μ SR signal appearing in the superconducting state of $\text{CaKFe}_4\text{As}_4$. The data were analyzed using the Kubo-Toyabe relaxation function [18] multiplied by an exponential decay function with a decay rate Λ ,

$$A(t) = A(0) \left\{ \frac{1}{3} + \frac{2}{3} (1 - a^2 t^2) \exp \left(-\frac{a^2 t^2}{2} \right) \right\} \exp(-\Lambda t), \quad (1)$$

where $A(0)$ is the initial asymmetry, and a and Λ are muon spin relaxation rates of the nuclear and electronic moments, respectively. Since we expect that the contribution from the nuclear moments will be similar above and below T_c , a was kept as a common parameter for all temperature data. The fits yield $a = 0.045(2) \mu\text{s}^{-1}$ which is very small and reflects the presence of random local fields arising from the nuclear moments within $\text{CaKFe}_4\text{As}_4$. Figure 1 (b) show that Λ is nearly temperature independent across T_c and therefore rules out the presence of any magnetic anomaly in the superconducting state of $\text{CaKFe}_4\text{As}_4$. The small values of Λ are consistent with the presence of diluted and randomly oriented electronic moments in this material. A 5 mT longitudinal field (LF) is sufficient to decouple the remaining moments completely (see Fig.1 (a)), which further suggests that these moments are static in nature. All the ZF- μ SR time spectra could be fitted with a single asymmetry function, implying that $\text{CaKFe}_4\text{As}_4$ is fully paramagnetic in the normal state.

Figure 2 shows the TF- μ SR time spectra collected at 1.6 and 35 K in a TF of 40 mT. As expected, muon spin depolarisation rate in the superconducting state (1.6 K data) is much stronger than in the normal state (35 K data) due to the spatial field modulation of the flux line lattice, formed in the mixed state of $\text{CaKFe}_4\text{As}_4$. All these responses can be described by an oscillatory term with a Gaussian envelope,

$$A^{TF}(t) = A(0) \exp \left(-\sigma^2 t^2 / 2 \right) \cos(\gamma_\mu \langle B \rangle t + \phi) + A_{bg}(0) \cos(\gamma_\mu B_{bg} t + \phi), \quad (2)$$

where $A(0)$ and $A_{bg}(0)$ are the initial asymmetries of the sample and background signals, $\gamma_\mu/2\pi = 135.5$ MHz/T is the muon gyromagnetic ratio [19], $\langle B \rangle$ and B_{bg} are the internal and background magnetic fields, ϕ is the initial phase of the muon precession signal, and σ is the Gaussian muon spin relaxation rate. σ represents the second moment of the internal field distribution. It is worthwhile to mention here that our background signals are very small due to the hematite slabs mounted immediately after the sample. Any muons missing the sample

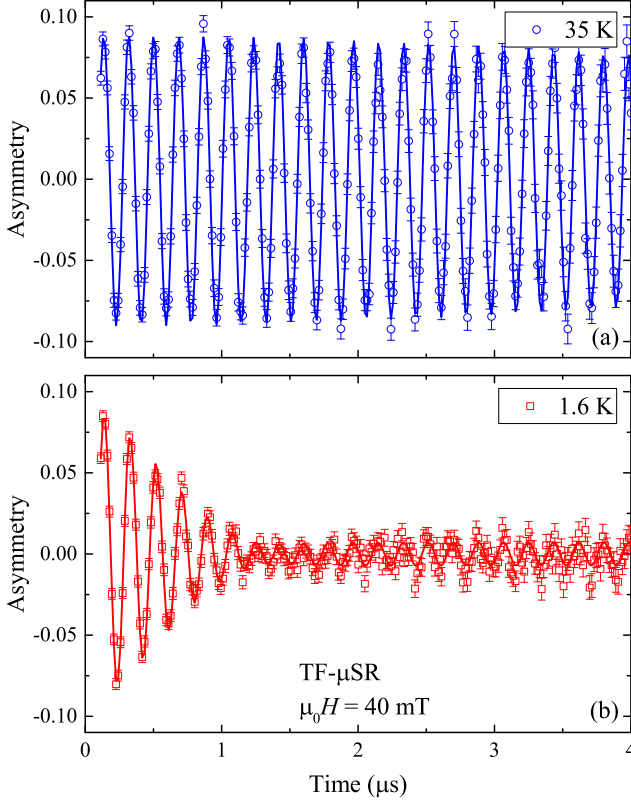


FIG. 2: (Color online) TF- μ SR time spectra of $\text{CaKFe}_4\text{As}_4$, collected at 1.6 and 35 K in a transverse field of 40 mT. The solid lines are the fits to the data using the Eq. 2.

implanted into the hematite slabs which then depolarize quickly within few nanoseconds and appear as an asymmetry loss in the TF- μ SR signals. A very small background signal most probably originates from a small number of muons hitting the Ag sample holder and is assumed to be non-relaxing over the muon time window, an assumption supported by ZF- μ SR.

Figure 3 (a) shows the temperature dependence of σ for $\text{CaKFe}_4\text{As}_4$ which exhibits a pronounced increase below T_c . Figure 3 (b) shows the expected diamagnetic shift below T_c in the form of internal magnetic field strength at the muon site in $\text{CaKFe}_4\text{As}_4$. σ can be expressed as $\sigma = (\sigma_{sc}^2 + \sigma_{nm}^2)^{\frac{1}{2}}$, where σ_{sc} is the superconducting contribution to the relaxation rate due to the inhomogeneous field variation across the flux line lattice and σ_{nm} is the nuclear magnetic dipolar contribution which is assumed to be temperature independent.

In light of Ginzburg-Landau treatment of the vortex state, Brandt [20] has shown that for a superconductor with a hexagonal vortex lattice and very high upper critical field, σ_{sc} is related to the penetration depth, λ by the simplified Brandt equation,

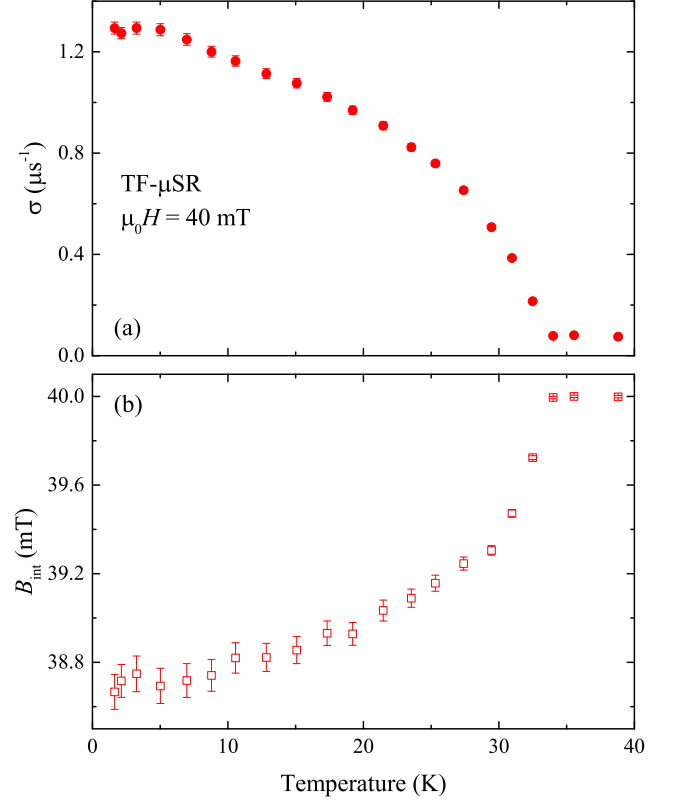


FIG. 3: (Color online) (a) Temperature dependence of the muon spin relaxation rate σ of $\text{CaKFe}_4\text{As}_4$. (b) Temperature dependence of the internal field strength of $\text{CaKFe}_4\text{As}_4$ for an applied field of 40 mT.

$$\frac{\sigma_{sc}(T)}{\gamma_{\mu}} = 0.06091 \frac{\Phi_0}{\lambda^2(T)}, \quad (3)$$

where $\Phi_0 = 2.068 \times 10^{-15}$ Wb is the flux quantum [20]. $\lambda^{-2}(T)$ is proportional to the effective superfluid density, $\rho_s \propto \lambda^{-2}$ and hence carries the information about the symmetry and size of a superconducting gap. Figure 4 shows the temperature dependence of λ^{-2} for $\text{CaKFe}_4\text{As}_4$. The fits to the $\lambda^{-2}(T)$ data were made using either a single gap or a combination of two gaps models using the following functional form [21, 22]:

$$\frac{\lambda^{-2}(T)}{\lambda^{-2}(0)} = \omega \frac{\lambda^{-2}(T, \Delta_1(0))}{\lambda^{-2}(0, \Delta_1(0))} + (1 - \omega) \frac{\lambda^{-2}(T, \Delta_2(0))}{\lambda^{-2}(0, \Delta_2(0))}, \quad (4)$$

where $\lambda(0)$ is the value of the penetration depth at $T = 0$ K, $\Delta_i(0)$ is the value of the i -th ($i = 1$ or 2) superconducting gap at $T = 0$ K and ω is the weighting factor of the first gap.

Each component of Eq. 4 can be expressed within the local London approximation ($\lambda \gg \xi$) [23, 24] as

$$\frac{\lambda^{-2}(T, \Delta_{0,i})}{\lambda^{-2}(0, \Delta_{0,i})} = 1 + \frac{1}{\pi} \int_0^{2\pi} \int_{\Delta(T, \varphi)}^{\infty} \left(\frac{\partial f}{\partial E} \right) \frac{EdEd\varphi}{\sqrt{E^2 - \Delta_i(T, \varphi)^2}}, \quad (5)$$

where $f = [1 + \exp(E/k_B T)]^{-1}$ is the Fermi function, φ is the angle along the Fermi surface, and $\Delta_i(T, \varphi) = \Delta_{0,i} \delta(T/T_c) g(\varphi)$, where $g(\varphi)$ describes the angular dependence of the gap. The temperature dependence of the gap can be approximated by the expression $\delta(T/T_c) = \tanh \left\{ 1.82 [1.018 (T_c/T - 1)]^{0.51} \right\}$ [21].

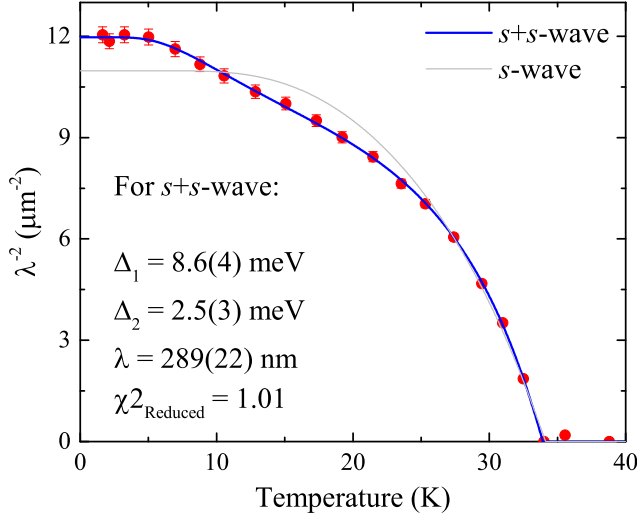


FIG. 4: (Color online) Temperature dependence of λ^{-2} for $\text{CaKFe}_4\text{As}_4$. The solid curves are the fits to the data using a single-gap s -wave and two-gap $s+s$ -wave models.

The solid curves shown in Fig. 4 are fits to the $\lambda^{-2}(T)$ data from $\text{CaKFe}_4\text{As}_4$ using a single gap s -wave and two-gap $s+s$ -wave models. For simplicity, we have not shown the fitted curves corresponding to anisotropic s - and $s+d$ -wave models in Fig. 4. All the fitted parameters are summarized in Table I. The two-gap $s+s$ -wave gap model gives a lower χ^2_{reduced} value than any other above mentioned models, and gives a much better fit to the data compared to the single-gap s -wave model with gap values of 8.6(4) and 2.5(3) meV and $\lambda(0) = 289(22)$ nm. Therefore it can be concluded that $\text{CaKFe}_4\text{As}_4$ is a multiple gap superconductor which is consistent with other layered Fe-based superconductors [5, 25–27]. Some other well-known examples of multi-gap superconductivity are represented by MgB_2 , NbSe_2 , and $\text{Lu}_2\text{Fe}_3\text{Si}_5$ [29–32]. The two-gap model, used here to analyze our final results, is a very simple approach to describe multiple superconducting gaps in the pairing symmetry data and has been used extensively in the past. For example, a similar model has also been used by Ch. Niedermayer *et al* to investigate the symmetry and values of the superconducting gaps in MgB_2 [28].

TABLE I: Fitted parameters to the $\lambda^{-2}(T)$ data of $\text{CaKFe}_4\text{As}_4$ using the different models as described in the text.

| Model | $g(\varphi)$ | Gap value (meV) |
|-----------------------|-----------------------|--|
| s -wave | 1 | $\Delta = 6.9(1)$ |
| $s+s$ -wave | 1 | $\Delta_1 = 8.6(4)$, $\Delta_2 = 2.5(3)$ and $\omega = 0.68(4)$ |
| anisotropic s -wave | $(s + \cos 4\varphi)$ | $\Delta = 7.0(1)$ with $s = 0.71(3)$ |
| $s+d$ -wave | $1, \cos(2\varphi) $ | $\Delta_1 = 10(1)$, $\Delta_2 = 6(1)$ and $\omega = 0.44(8)$ |

The superconducting gap values obtained from the two-gap model fits are in excellent agreement with the reported values obtained from the STM measurements for this material [13] and also consistent with other layered Fe-based superconductors, especially from the μSR and ARPES measurements of optimally doped $(\text{Ba}, \text{K}, \text{Rb})\text{Fe}_2\text{As}_2$ system [33, 34]. These are, however, more than double the values reported from the TDR measurements of $\text{CaKFe}_4\text{As}_4$ [13]. Our finding of two superconducting gaps in $\text{CaKFe}_4\text{As}_4$ is not unsurprising and is very much consistent with other members of Fe-based superconductors. It is now an universal phenomena across all Fe-based superconductors, apart from a small number of exceptions, such as the highly electron-doped regime of $(\text{Ba}, \text{K}, \text{Rb})\text{Fe}_2\text{As}_2$ system.

In summary, ZF- and TF- μSR measurements have been performed on $\text{CaKFe}_4\text{As}_4$, a member of the newly discovered family of high- T_c Fe-based superconductors $A_e\text{AFe}_4\text{As}_4$ ($A_e = \text{Ca}, \text{Sr}, \text{Eu}$ and $A = \text{K}, \text{Rb}, \text{Cs}$). ZF- μSR data confirm that there is no magnetic anomaly in the superconducting ground state of $\text{CaKFe}_4\text{As}_4$. The temperature dependence of the magnetic penetration depth is found to be strongly compatible with a two-gap $s+s$ -wave model with gap values, $\Delta_1(0) = 8.6(4)$, $\Delta_2(0) = 2.5(3)$ meV with weighting factor $\omega = 0.68(4)$ to the large gap. We obtain the penetration depth, $\lambda(0) = 289(22)$ nm. Our results show that $\text{CaKFe}_4\text{As}_4$ is a fully developed nodeless multi-gap superconductor and all the fitted gap parameters are very similar to the optimally doped $(\text{Ba}, \text{K}, \text{Rb})\text{Fe}_2\text{As}_2$ systems. Further studies are in progress to explore the pressure evolution of the symmetry of the superconducting gaps in this materials.

The μSR experiments were performed at the ISIS Pulsed Neutron and Muon Source, STFC Rutherford Appleton Laboratory, (STFC, United Kingdom).

* Corresponding author: pabitra.biswas@stfc.ac.uk

- [1] Y. Kamihara, T. Watanabe, M. Hirano, and H. Hosono, J. Am. Chem. Soc. **130**, 3296 (2008).
- [2] F.-C. Hsu, J.-Y. Luo, K.-W. Yeh, T.-K. Chen,

- T.-W. Huang, P. M. Wu, Y.-C. Lee, Y.-L. Huang, Y.-Y. Chu, D.-C. Yan, and M.-K. Wu, *Proc. Natl. Acad. Sci. USA* **105**, 14262 (2008).
- [3] G. R. Stewart, *Rev. Mod. Phys.* **83**, 1589 (2011).
- [4] X. Chen, P. Dai, D. Feng, T. Xiang, F. C. Zhang, *Natl. Sci. Rev.* **1**, 371 (2014).
- [5] J. Paglione and R. L. Greene, *Nat. Phys.* **6**, 645 (2010).
- [6] J. G. Bednorz, and K. A. Muller, *Z. Physik B* **64**, 189 (1986).
- [7] A. Iyo, K. Kawashima, T. Kinjo, T. Nishio, S. Ishida, H. Fujihisa, Y. Gotoh, K. Kihou, H. Eisaki, and Y. Yoshida, *J. Am. Chem. Soc.* **138**, 3410 (2016).
- [8] W. R. Meier, T. Kong, U. S. Kaluarachchi, V. Taufour, N. H. Jo, G. Drachuck, A. E. Böhrer, S. M. Saunders, A. Sapkota, A. Kreyssig, M. A. Tanatar, R. Prozorov, A. I. Goldman, S. L. Bud'ko, and P. C. Canfield, *arXiv:1605.05617* (2016).
- [9] Y. Liu, Y.-B. Liu, Z.-T. Tang, H. Jiang, Z.-C. Wang, A. Ablimit, W.-H. Jiao, Q. Tao, C.-M. Feng, Z.-A. Xu, and G.-H. Cao, *arXiv:1605.04396* (2016).
- [10] Y. Liu, Y.-B. Liu, Q. Chen, Z.-T. Tang, W.-H. Jiao, Q. Tao, Z.-A. Xu, and G.-H. Cao, *arXiv:1605.09007* (2016).
- [11] T. Kong, F. F. Balakirev, W. R. Meier, S. L. Budko, A. Gurevich, and P. C. Canfield, *arXiv:1606.02241* (2016).
- [12] M. M. Altarawneh, K. Collar, C. H. Mielke, N. Ni, S. L. Budko, and P. C. Canfield, *Phys. Rev. B* **78**, 220505 (2008).
- [13] K. Cho, A. Fente, S. Teknowijoyo, M. A. Tanatar, T. Kong, W. Meier, U. Kaluarachchi, I. Guillamón, H. Suderow, S. L. Budko, P. C. Canfield, and R. Prozorov, *arXiv:1606.06245* (2016).
- [14] D. Mou, T. Kong, W. R. Meier, F. Lochner, L.-L. Wang, Q. Lin, Y. Wu, S. L. Budko, I. Eremin, D. D. Johnson, P. C. Canfield, A. Kaminski, *arXiv:1606.05643* (2016).
- [15] www.isis.stfc.ac.uk/instruments/musr/.
- [16] www.mantidproject.org.
- [17] A. Suter, and B. M. Wojek, *Physics Procedia* **30**, 69 (2012).
- [18] R. Kubo, *Hyperfine Interact.* **8**, 731 (1981).
- [19] J. E. Sonier, J. H. Brewer, and R. F. Kiefl, *Rev. Mod. Phys.* **72**, 769 (2000).
- [20] E. H. Brandt, *Phys. Rev. B* **68**, 054506 (2003).
- [21] A. Carrington, and F. Manzano, *Physica C* **385**, 205 (2003).
- [22] H. Padamsee, and J. E. Neighbor, and C. A. Shiffman, *J. Low Temp. Phys.* **12**, 387 (1973).
- [23] M. Tinkham, *Introduction to Superconductivity* (McGraw-Hill, New York, 1975).
- [24] R. Prozorov, and R. W. Giannetta, *Supercond. Sci. Technol.* **19**, R41 (2006).
- [25] R. Khasanov, K. Conder, E. Pomjakushina, A. Amato, C. Baines, Z. Bukowski, J. Karpinski, S. Katrych, H.-H. Klauss, H. Luetkens, A. Shengelaya, N. D. Zhigadlo, *Phys. Rev. B* **78**, 220510(R) (2008).
- [26] P. K. Biswas, G. Balakrishnan, D. McK. Paul, C. V. Tomy, M. R. Lees, A. D. Hillier, *Phys. Rev. B* **81**, 092510 (2010).
- [27] P. K. Biswas, A. Krzton-Maziopa, R. Khasanov, H. Luetkens, E. Pomjakushina, K. Conder, and A. Amato, *Phys. Rev. Lett.* **110**, 137003 (2013).
- [28] Ch. Niedermayer, C. Bernhard, T. Holden, R. K. Kremer, and K. Ahn, *Phys. Rev. B* **65**, 094512 (2002).
- [29] H. J. Choi, D. Roundy, H. Sun, M. L. Cohen, and S. G. Louie, *Nature (London)* **418**, 758 (2002), and references therein.
- [30] T. Yokoya, T. Kiss, A. Chainani, S. Shin, M. Nohara, H. Takagi, *Science* **294**, 2518 (2001).
- [31] Y. Nakajima, T. Nakagawa, T. Tamegai, and H. Harima, *Phys. Rev. Lett.* **100**, 157001 (2008).
- [32] P. K. Biswas, G. Balakrishnan, D. McK. Paul, M. R. Lees, and A. D. Hillier, *Phys. Rev. B* **83**, 054517 (2011).
- [33] R. Khasanov, D. V. Evtushinsky, A. Amato, H.-H. Klauss, H. Luetkens, Ch. Niedermayer, B. Büchner, G. L. Sun, C. T. Lin, J. T. Park, D. S. Inosov, and V. Hinkov, *Phys. Rev. Lett.* **102**, 187005 (2009).
- [34] Z. Guguchia, A. Amato, J. Kang, H. Luetkens, P.K. Biswas, G. Prando, F. von Rohr, Z. Bukowski, A. Shengelaya, H. Keller, E. Morenzoni, Rafael M. Fernandes and R. Khasanov, *Nat. Commun.* **6** 8863 (2015).